

The gluon propagator close to criticality

Axel Maas,^{1,*} Jan M. Pawłowski,^{2,3,†} Lorenz von Smekal,^{4,‡} and Daniel Spielmann^{2,3,§}

¹*Theoretical-Physical Institute, Friedrich-Schiller-University Jena, Max-Wien-Platz 1, D-07743 Jena, Germany*

²*Institute for Theoretical Physics, University of Heidelberg,
Philosophenweg 16, D-69120 Heidelberg, Germany*

³*ExtreMe Matter Institute EMMI, GSI, Planckstr. 1, D-64291 Darmstadt, Germany*

⁴*Institut für Kernphysik, Technische Universität Darmstadt,
Schlossgartenstr. 2, D-64289 Darmstadt, Germany*

(Dated: February 18, 2022)

There are good reasons that the deconfinement phase transition of pure Yang-Mills theory at finite temperature should also be reflected in the behavior of gauge-fixed gluonic correlation functions. Understanding this in detail would provide another important example of how physical information can be extracted from gauge-dependent correlations, which is not always obvious. Therefore, herein we study the behavior of the Landau-gauge gluon propagator of pure $SU(2)$ across the phase transition in 2+1 and 3+1 dimensions in order to assess to what extent the corresponding critical behavior is reflected in these correlations. We discuss why it should emerge from a continuum perspective and test our expectations in lattice simulations. A comparison with $SU(3)$ furthermore reveals quite clear indications for a sensitivity of the gluon propagator to the order of the transition.

PACS numbers: 12.38.Aw, 12.38.Lg, 11.15.Ha, 12.38.Mh, 25.75.Nq

I. INTRODUCTION

Our knowledge of even the most basic characteristic features of the QCD phase diagram is still rather uncertain. A rich structure of possible phases and transitions between them is being discussed in various regions, see, e.g. [1–3]. Understanding how these phase transitions manifest themselves both theoretically and experimentally in a joint effort is the great challenge of strongly interacting matter research.

One of the well established properties of QCD with 2+1 flavors of dynamical quarks is a crossover at vanishing chemical potential in a temperature range of about 150–180 MeV, e.g. [4–7]. However, many observables nevertheless appear to reflect the deconfinement phase transition that would occur if all quarks were sufficiently heavy. In fact, whether and where in the so-called Columbia plot the change from a genuine phase transition to a crossover occurs might still change when going beyond QCD as an isolated theory. In particular, if one also considers the quarks' fractional electric charges and couplings to more than one gauge group as in the Standard Model, a center-like symmetry reemerges which can break at the transition as in the quenched case [8].

This finite-temperature deconfinement phase transition of the pure $SU(N)$ Yang-Mills theory in $d + 1$ dimensions follows the Z_N symmetry breaking pattern of a d -dimensional q -state Potts model with $q = N$. It is of second order for $N = 2$ (Ising universality class) in

$d = 2$ and 3 and for $N = 3$ in $d = 2$. The self-duality of the 2-dimensional Potts models thereby manifests itself in the free energies of the confining electric fluxes being mirror images around criticality of those of center-vortex ensembles with twisted boundary conditions [9–11].

Another tool to determine the dynamics of order parameters for the Yang-Mills phase transition, in particular the Polyakov loop, the chiral condensate and to some extent thermodynamic bulk properties, have been gauge-fixed correlation functions, in particular in the Landau gauge. While it has been known since decades how the chiral phase transition and in particular its critical properties manifest themselves directly in the gauge-fixed quark correlation functions, it has only recently become clear how to compute the non-perturbative effective potential of deconfinement order parameters from the gauge-fixed propagators [7, 12–18]. These analyses entail that already the gauge-fixed propagators carry the critical properties of the confinement-deconfinement phase transition, which has been used explicitly in [13]. These findings have also been studied using lattice simulations, see in particular [18, 19], though systematic errors are still a matter of ongoing research [18–22].

In the present paper we extend these investigations. We first review in Section II how critical properties of the phase transition are incorporated in the gauge-fixed correlation functions. We argue that the gluon propagator should be directly sensitive to the phase transition and, in particular, that it should reflect critical scaling. In Section III the behavior expected from these arguments is compared to results from lattice simulations in three and four dimensions for $SU(2)$ Yang-Mills theory. In both cases the phase transitions are of second order, but one should be able to distinguish the different critical exponents corresponding the $2d$ and $3d$ Ising universality classes, respectively. We also briefly revisit the first-

*Electronic address: axelmaas@web.de

†Electronic address: J.Pawłowski@thphys.uni-heidelberg.de

‡Electronic address: lorenz.smekal@physik.tu-darmstadt.de

§Electronic address: D.Spielmann@ThPhys.Uni-Heidelberg.de

order case of four-dimensional $SU(3)$ Yang-Mills theory to assess the sensitivity of the gluon propagator to the order of the transition in Section IV. Our summary and conclusion are given in Section V. Some additional results on the momentum dependence of the propagators are deferred to Appendix A, while an extended discussion of the systematic and statistical errors is given in Appendices B and C, respectively.

II. CRITICAL BEHAVIOR AND THE GLUON PROPAGATOR

The second-order finite-temperature deconfinement phase transitions of $SU(2)$ Yang-Mills theory in four, and both $SU(2)$ and $SU(3)$ in three dimensions, are characterized by correlation lengths which diverge at the critical temperature in the infinite volume limit. As a consequence, only the long-range properties of the theory matter near criticality. These are determined by symmetries and dimensionality of the system, and the concepts of universality and scaling apply. The second-order $SU(N)$ cases belong to Potts/Ising universality classes in two and three dimensions as mentioned above. In particular, the $SU(2)$ Yang-Mills theories in three and four dimensions that we are mainly interested in here, belong to the classes of the two-dimensional and three-dimensional Ising models, respectively.

Critical behavior manifests itself in singularities of thermodynamic functions at the critical temperature T_c (and vanishing external field). In particular, these singularities show as characteristic non-integer powers of the reduced temperature

$$t = \left(\frac{T}{T_c} - 1 \right). \quad (1)$$

The critical exponents in these power laws only depend on symmetry-breaking pattern and dimension, and are thus a characteristic feature of a universality class. Scaling and hyper-scaling (in four dimensions or less) entail that all critical exponents can be expressed in terms of two independent ones, say ν and η . The first is the critical exponent of the diverging correlation length ξ , i.e.,

$$\xi \propto |t|^{-\nu}, \quad (2)$$

close to a second-order phase transition. The second is defined from the (in general renormalization-group-dependent) connected propagator $G(p)$ of the order parameter, whose zero momentum contribution defines the susceptibility which diverges with exponent γ ,

$$G(0) \propto |t|^{-\gamma}, \quad \text{with } \gamma = \nu(2 - \eta). \quad (3)$$

In the broken phase, an order parameter M scales with the exponent β ,

$$M(t) \propto |t|^\beta \quad \text{with } \beta = \frac{1}{2}\nu(d - 2 + \eta). \quad (4)$$

Usually β is bound by its mean field value, i.e. $\beta \leq 1/2$, and the derivative of $M(t)$ with respect to t therefore diverges at the critical temperature.

A natural order parameter for confinement is provided by the Polyakov loop,

$$L(\vec{x}) = \frac{1}{N_c} \text{tr P} \exp \left(ig \int_0^{1/T} d\tau A_0(\tau, \vec{x}) \right). \quad (5)$$

It depends on the zero component A_0 of the gauge field, and its correlation length is inversely related to the string tension, i.e., $\xi_- = T/\sigma(T)$ for $T < T_c$. Therefore, with second-order transition, $\sigma \propto (-t)^\nu$ for $t \rightarrow 0^-$.¹

In a gauge-fixed approach the theory is described in terms of, in general, gauge-dependent correlation functions, i.e. N -point functions of the gauge field. These correlation functions have to contain the information about the physics at criticality, even though they change under gauge transformations.

Indeed it has been shown how to extract the expectation value of the (logarithm of the) Polyakov loop from the gauge-fixed propagators in general gauges in terms of the full effective potential V_{eff} of $\langle A_0 \rangle$ [12–14]. The value of $\langle A_0 \rangle$ at the minimum of V_{eff} directly relates to the expectation values of the eigenvalues of the (logarithm of the) Polyakov loop, it is gauge invariant and also provides an order parameter. Other recent examples are dual condensates [24–28], which can likewise be computed from gauge-fixed correlation functions [15–18, 29], and in the quenched case determine the Polyakov loop directly.

In [12, 14] the potential has been computed in Landau gauge; the critical temperature agrees well with lattice results. In [13] the same result was obtained within a computation in Polyakov gauge, a necessary requirement for the results to be gauge-independent as they must be. Moreover it has been verified that in $SU(2)$ the potential and hence the order parameter does indeed show the scaling of the Ising universality class.

An interesting consequence of these computations and the related formal analysis is that the gauge-fixed propagators necessarily also show critical scaling. Here we briefly review the corresponding results in [12–14]. In [12] it has been shown that the effective potential of $\langle A_0 \rangle$ in a general gauge can be computed solely from the ghost and gluon propagators in the constant background \bar{A}_0 :

$$\begin{aligned} \partial_k V_{\text{eff},k}(\bar{A}_0) &= \frac{1}{2} \text{Tr} \langle A_\mu^a A_\nu^b \rangle_{\bar{A}_0} \partial_k R_{k,\nu\mu}^{ba} \\ &\quad - \frac{1}{2} \text{Tr} \langle \bar{C}^a C^b \rangle_{\bar{A}_0} \partial_k R_k^{ba}, \end{aligned} \quad (6)$$

¹ Above T_c , the Polyakov-loop correlation length ξ_+ is related to the dual string or interface tension $\bar{\sigma} \propto (\xi_+)^{1-d}$, a well-defined order parameter for center-symmetry breaking [23]. With second-order transition, $\bar{\sigma} \propto t^\mu$ for $t \rightarrow 0^+$, and (hyper-scaling) $\mu = (d - 1)\nu$.

where k is an infrared cut-off scale implemented by the regulator R_k^{ab} in the functional renormalization group equations. At large cut-off scales the effective potential vanishes. Hence, integrating the above equation (6) from the trivial potential at $k \rightarrow \infty$ to $k = 0$ provides us with $V_{\text{eff}}(\bar{A}_0) = V_{\text{eff},k=0}(\bar{A}_0)$ the full non-perturbative effective potential of $\langle A_0 \rangle$.

Since $V_{\text{eff}}(\bar{A}_0)$ is the potential of the order parameter $\langle \log L \rangle$, it has to show critical scaling (if the transition is of second order). Consequently, also the propagators will be sensitive to critical scaling, in general.

The above setting even allows us to extract the scaling of the longitudinal gluon. Its propagator schematically is of the form,

$$\langle A_L A_L \rangle_{\bar{A}_0} = \Pi_L \frac{1}{(-\bar{D}_0^2 + \bar{p}^2) Z_L} \Pi_L, \quad (7)$$

where Π_L stands for the projection operator longitudinal to the heatbath in the presence of the background \bar{A}_0 , and $i\bar{D}_0 = p_0 + g\bar{A}_0$. The prefactor $Z_L = Z_L(-\bar{D}_0^2, \bar{p}^2; \bar{A}_0)$ depends on \bar{A}_0 , \bar{D}_0^2 and \bar{p}^2 separately and reduces to the well-known longitudinal (inverse) Landau gauge dressing function for $\bar{A}_0 = 0$.

The solution a_0 of the equations of motion for \bar{A}_0 is the order parameter related to $\langle \log L \rangle$ and derives from

$$\left. \frac{\partial V_{\text{eff}}}{\partial \bar{A}_0} \right|_{\bar{A}_0=a_0} = 0. \quad (8)$$

Hence it scales according to (4), and the effective potential also shows critical scaling, i.e.

$$\frac{\partial^2 V_{\text{eff}}}{\partial \bar{A}_0^2}(a_0) \propto |t|^\gamma. \quad (9)$$

with $\gamma = \nu(2-\eta)$, see (3). Up to possible dependencies on the background field, the inverse longitudinal gluon propagator is proportional to (9), $\langle A_L A_L \rangle^{-1} \propto \partial^2 V_{\text{eff}} / \partial \bar{A}_0^2$. In other words, the mass gap is given by the curvature of $V_{\text{eff}}(\bar{A}_0)$ in (9), and hence determines the singular behavior of the gluon propagator at vanishing frequency and momentum, i.e.

$$\langle A_L A_L \rangle_{\bar{A}_0=a_0}(p=0) \propto |t|^{-\gamma}. \quad (10)$$

We conclude that at least the longitudinal or electric propagator (7) scales as the propagator of an order parameter, see (3). In [13] this has in fact been used to determine the critical scaling directly from the longitudinal gluon propagator.

Note however, that a similar analysis cannot be made for transverse gluons and ghosts. This is due to the fact that their inverse propagators contain no \bar{A}_0 -derivatives and hence no dependence on the curvature term in (9). Consequently, we cannot infer from this simple argument whether one should see critical scaling in the transverse gluon and ghost propagators or not. However, it is suggestive that it at best arises in sub-leading order, that is,

that singularities might appear in higher T -derivatives. This is supported by lattice results, see [18–20, 30] and appendix C.

Now we turn to lattice Landau gauge and, in particular, discuss the differences of simulations there to the background Landau gauge scenario used above. The screening mass of a two-point correlation function, the propagator $D(p)$, defined as

$$M_s = \frac{1}{\sqrt{D(0)}}, \quad (11)$$

is a candidate for critical behavior. Note that the corresponding pole mass [30], if it exists, will in general only be sensitive to correlation lengths up to its inverse size. Since all results available so far [30] seem to exclude a zero pole mass of the gluons, it is therefore to be expected that the pole mass will not exhibit critical behavior.

The temperature-dependence of the electric and magnetic gluon propagators and the ghost propagator in lattice Landau gauge has been investigated previously, for details see [18–22, 31–39]. One observes that only the electric propagator is sensitive to the phase transition [18, 19, 22]. However, the available lattice data do not yet allow to draw firm conclusions about a possible scaling behavior at criticality. Nevertheless, the susceptibility χ^E defined as the temperature derivative of its screening mass M_s^E ,

$$\chi^E = \frac{\partial M_s^E}{\partial T},$$

is sufficiently sensitive to determine the phase transition temperature within the systematic errors, see [18] and Appendix B.

The aim of the present investigation is the further assessment of the critical behavior. This will be performed using lattice simulations in three and four dimensions for the gauge group $SU(2)$. In four dimensions, for this purpose, a significantly refined temperature mesh and increased statistics were used compared to the previous study [18]. The three-dimensional system, investigated here for the first time, has the advantage, compared to the four-dimensional one, that the expected critical exponents are larger, and therefore the signal might be stronger.

In lattice Landau gauge, naively, one would expect a similar behavior as for the background Landau gauge discussed above. However, the two differ in at least one important qualitative aspect. All currently employed practical implementations of the lattice Landau gauge, including the one used herein, exhibit a screening mass. Given its non-perturbative origin and appearance in a gauge-fixed correlator, it will be referred to as a Gribov mass [40]², m_{gribov} . This mass is present at all temper-

² Note that in the original work [40] the so defined screening mass was infinite.

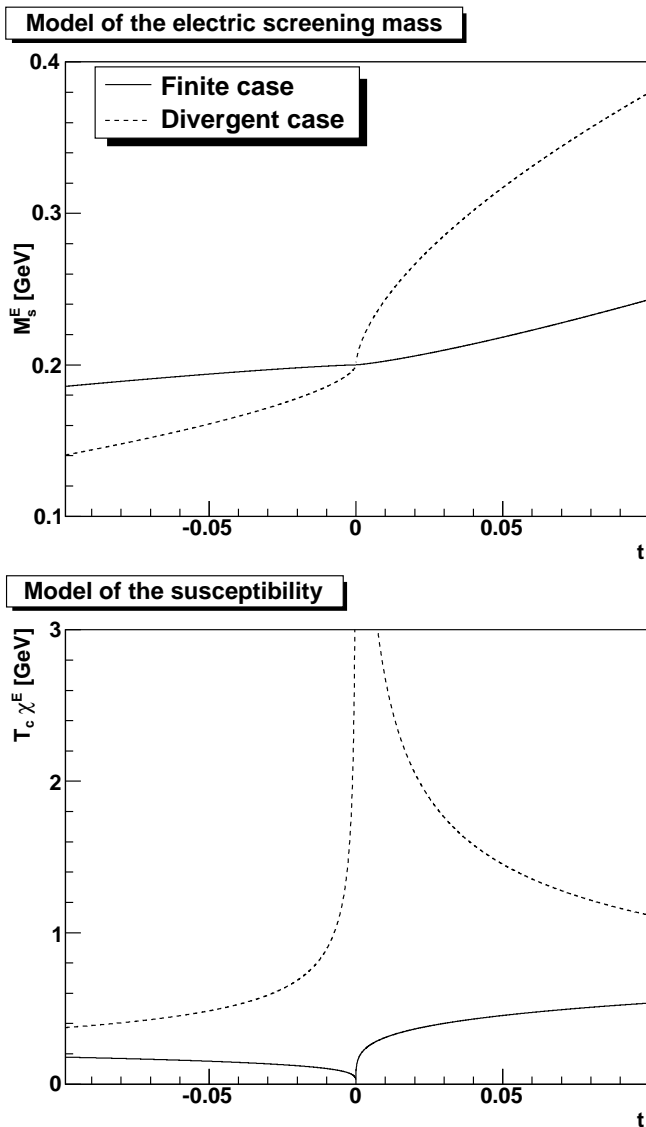


FIG. 1: Cartoon of the electric screening mass and susceptibilities of the form (12) and (13), with critical exponents $\gamma/2$ (divergent case) and γ (finite case) with $\gamma = 1.2372(5)$, i. e., with the 3-dimensional Ising universality class. The non-universal constants are $m_{\text{gribov}} = 0.2$ GeV, $a = -1/4$ GeV and $b = 3/4$ GeV.

atures and hence interferes with critical scaling. This entails that the inverse propagator can still have a mass-gap at criticality. It is important to emphasize that the effective potential V_{eff} for the order parameter a_0 in such a gauge still satisfies (6). Hence, the propagators must reflect critical scaling nevertheless. This implies that the screening mass M_s^E of the electric propagator in (11) contains both, a regular Gribov mass contribution as well as a singular critical one. From Eq. (6) one concludes that the critical contribution is determined by the exponent γ . Unfortunately, this general argument is not sufficient to disentangle the two contributions in a unique way. The

two perhaps most natural candidates to explore at least as approximate descriptions near criticality might be to either simply add the two mass contributions directly, i.e.

$$M_s^E(t) = m_{\text{gribov}} + a_{\pm} |t|^{\gamma/2}, \quad (12)$$

where $a_+ = a$ is a non-universal coefficient for temperature $t > 0$ and $a_- = b$ for temperatures $t < 0$; or, alternatively, add two corresponding self-energy contributions to the inverse propagator which would lead to a sum of squares for the total mass, i.e.

$$M_s^E(t) = \sqrt{m_{\text{gribov}}^2 + a_{\pm}^2 |t|^{\gamma}}. \quad (13)$$

A simply testable criterion to at least discriminate these two cases is provided by the corresponding susceptibilities χ^E which near criticality in the first case (12) behaves as $\chi^E \propto |t|^{\gamma/2-1}$, while with (13), $\chi^E \propto |t|^{\gamma-1}$. For $1 < \gamma < 2$, in the $2d$ and $3d$ Ising universality classes one has $\gamma = 7/4 = 1.75$ and $\gamma = 1.2372(5)$, respectively [41]. This implies that (12) leads to a susceptibility $\chi^E = \partial_t M_s^E$ which would diverge at the critical temperature (in the infinite volume limit), while (13) would lead to a vanishing one. This is illustrated by a cartoon of the four-dimensional case in Figure 1.

While there will of course neither be a divergence nor a strict zero in χ^E in a finite volume, the lattice results clearly favor an enhancement of χ^E near T_c corresponding to (12) rather than a suppression, as can be seen from comparing the cartoon in Figure 1 with Figures 2 and 4 below. So we conclude that (13) can relatively safely be ruled out. A more conclusive study of the expected behavior based on a self-consistency analysis of (6) would be clearly desirable but will be postponed to future work.

Furthermore, because the Gribov mass itself is significantly volume dependent [30, 42–45], it is not possible at present to clearly identify the critical behavior in the electric screening mass or its temperature derivative from a finite-size-scaling analysis of lattice results. The Gribov mass creates a mass gap whose volume dependence especially at criticality is yet to be determined. A significant amount of different volumes, and possibly discretizations, will be necessary to disentangle the two intertwined finite-volume effects on the electric screening mass, from critical scaling and from the Gribov mass, requiring substantially more resources than presently available to us.

Finally, it should be noted that the ansätze (12) and (13) are expected to be only valid in the critical region. The Gribov mass in these fits will therefore not coincide with the one at zero temperature, as further, sub-leading temperature-dependent contributions are neglected.

III. LATTICE RESULTS

The gluon propagator is determined using standard lattice methods, for details see [19, 46]. We use the minimal Landau gauge [30] with the implications discussed

in Section II. In particular, the gluon propagator exhibits a finite Gribov screening mass already at zero temperature, while the ghost behaves essentially tree-level-like [42–45, 47, 48]. In four dimensions, in addition to the data from [18], further results using a finer discretization at the price of smaller physical volumes, are used. In three dimensions, two different discretizations are used as well. For the main purpose of this work only the electric screening mass is of importance. For completeness, also the finite momentum results are reported, but relegated to Appendix A.

For setting the scale a string tension of $(440 \text{ MeV})^2$ has been used, based on the $a(\beta)$ values determined in [49] for three dimensions and in [50] for four dimensions. This particular value was chosen to ensure comparability to the previous investigations [18, 19]. The critical β values are taken from [51] for three dimensions and from [50] for four dimensions. A discussion of systematic effects due to the scale setting can be found in Appendix B 1.

A. Three dimensions

The results for the electric screening mass, as well as its susceptibility in three dimensions are shown in Figure 2. It is clearly visible that the maximum of the susceptibility marks the critical temperature, which has been determined independently using analyses of the free energy and quantities derived from it [50, 51]. Furthermore, a sizable volume scaling is seen for the smaller spatial volumes with $N_t = 4$ time slices. For the largest spatial extent the peak in the susceptibility only becomes somewhat sharper, but not significantly higher. This might be due to the mixing with the Gribov mass as discussed in Section II. Note, however, that the singular contribution to $\chi^E = \partial_t M_s^E \propto |t|^{\gamma/2-1}$ from our model (12) would predict a finite-size L scaling of the maximum as $\chi_{\text{max}}^E \propto L^{(1-\gamma/2)/\nu} = L^{1/8}$ for three-dimensional $SU(2)$, corresponding to a factor $2^{1/8}$ or about only 9% increase with doubling the spatial lattice size which is still within errors. Furthermore, increasing N_t from 4 to 6, which effectively reduces the physical L for equal spatial lattice sizes by $2/3$, we observe that the results remain qualitatively unchanged, at least for the two values checked here. The details might still be influenced by lattice artifacts.

We reiterate that the screening mass, which is (semi)positive by definition, is non-zero at the phase transition. Moreover, because the peak in its temperature derivative χ^E marks the phase transition, the screening mass does not have a minimum there, but a point of inflection.³ It is also well established that there is a finite

³ From the coarser temperature resolution in [18] it was suggested that the transition occurred at the maximum of the electric gluon propagator at zero momentum, i.e. for minimal M_s^E , which is slightly off. However, this merely implies that the phase transition temperature should be set to the peak in the susceptibility

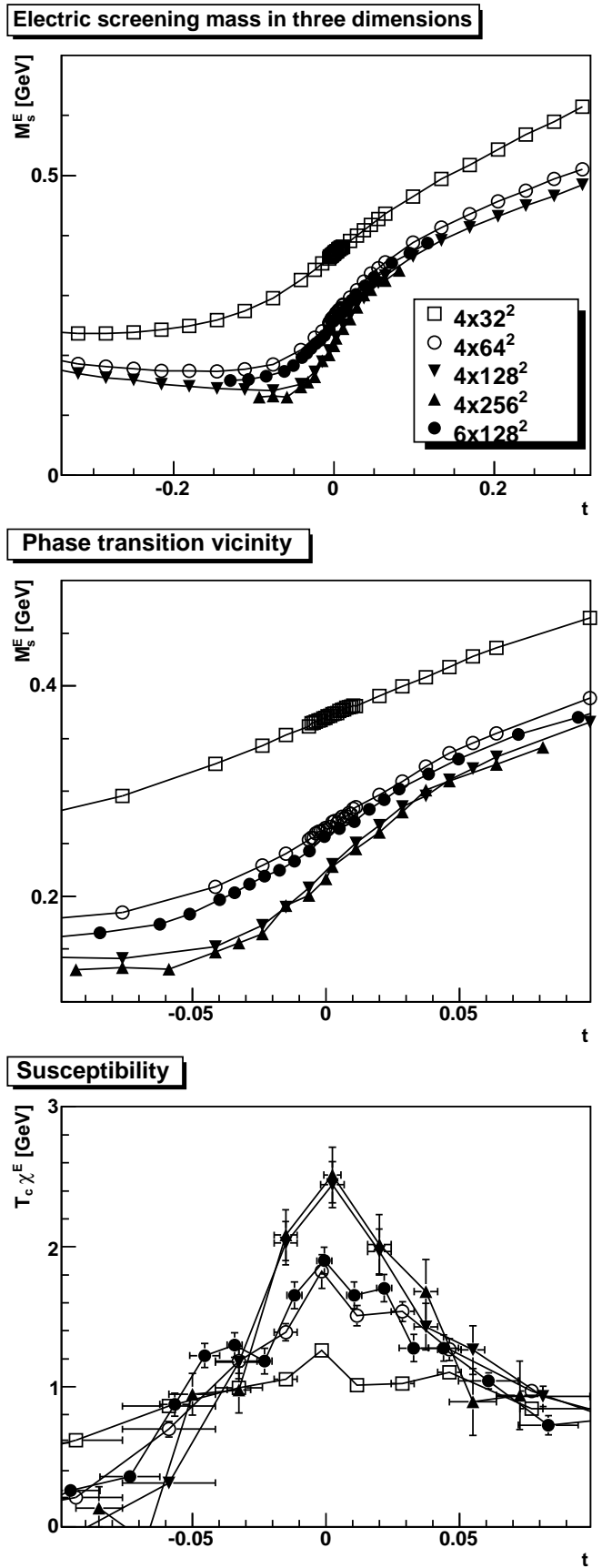


FIG. 2: The electric screening mass (top panel and zoomed in in the phase transition region in the middle panel) as a function of the reduced temperature for various lattice sizes. The bottom panel shows the corresponding susceptibility, where some temperature points have been dropped to reduce the statistical errors.

screening mass in minimal Landau gauge at zero temperature [44]. The possibility that it remains constant throughout all temperatures up to the phase transition, and that it starts to increase abruptly there, would imply that the non-universal coefficient $a_- = b = 0$ and is included here. For our fits we thus assume a constant contribution corresponding to a Gribov mass introduced by the gauge-fixing, which should be temperature-independent, to which we add a form resembling a critical behavior as in (12). Subleading contributions around criticality will be neglected, leading to the Ansatz for the screening mass,

$$M_s^E(t) = m_{\text{gribov}} + \theta(t) a t^{\frac{\gamma_+}{2}} + \theta(-t) b (-t)^{\frac{\gamma_-}{2}}, \quad (14)$$

where we have furthermore introduced independent exponents γ_+ and γ_- above and below T_c in order to assess to what extent the results are consistent with a unique $\gamma_+ = \gamma_-$. As a side remark note that the Ansatz (14) for small t in principle also includes the form in (13) for which one should obtain $\gamma_+ = \gamma_- = 2\gamma$.

Performing the fits in the reduced-temperature interval $[-0.1, 0.1]$ yields the results shown in table I. An example of the quality of the fit is shown in Figure 3. There are a number of observations:

First, the fit form (14) describes the screening mass rather accurately, and within the statistical errors also the susceptibility in a satisfactory way. The resulting exponents are all in the range $1 < \gamma < 2$ (and thus inconsistent with (13)), but they do not agree with one another very well, which is only slightly improved if the fit interval is further reduced, assuming a smaller critical region.

Given that the fits provide a rather good description of both the screening mass and the susceptibility there are a number of possible reasons for the observed non-singularity in the data itself. The first is that the volumes are just too small and the discretization too coarse to be close enough to a critical behavior. Given that the critical behavior is well visible on comparable lattices for other observables [51], this appears at first glance to be a rather unlikely explanation. However, it is possible that the electric gluon propagator lags significantly in the development of the critical behavior behind those other observables. Indeed, the gluon propagator requires already at zero temperature very large volumes to reach even its qualitative infinite-volume behavior [42–45]. This appears to be true also at finite temperature [19, 21]. Therefore this appears to be a possible explanation.

The second possibility is that the critical region is very narrow. Then it would be necessary to investigate the region around the critical temperature with a much finer mesh. In this case also significantly enhanced statistics would be necessary, since the numerical derivative for

χ^E instead. Otherwise the results of [18] remain unchanged.

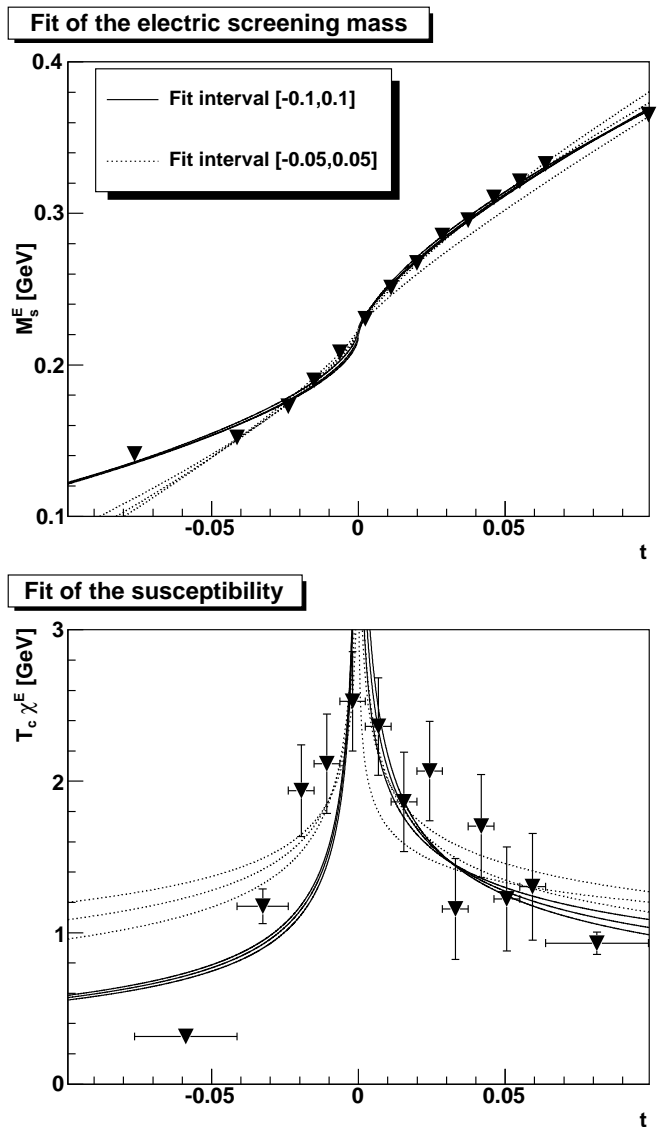


FIG. 3: The quality of the fits compared to the data from the 4×128^2 lattice. The standard fit uses the values from Table I. As an alternative, a fit using only a more restricted reduced temperature interval $[-0.05, 0.05]$ is also shown (dotted line), which yields $\gamma_- = 1.52_{-9}^{+10}$ and $\gamma_+ = 1.61_{-14}^{+12}$. Fits have been performed on the screening mass using all data points, and the derivatives have then been calculated analytically. The error bands are also shown.

the determination of the susceptibility requires that the statistical error must be much smaller than the distance between two points.

Finally, it is of course still possible that the electric gluon propagator simply does not show critical behavior. At the moment this cannot entirely be excluded, despite the general continuum arguments in favor given in Section II. This could be due, e.g. to a more complicated interference with the Gribov mass than the two possibilities considered in (12) and (13). An alternative possibility will be discussed in Section III C below. How-

TABLE I: The fit parameters for the fit (14) for the three-dimensional case. For the determination and placement of the statistical errors see Appendix C. Only the change in the last digits is indicated. See Appendix B for a discussion of systematic errors.

| Lattice | m_{gribov} [GeV] | a [GeV] | b [GeV] | γ_+ | γ_- |
|------------------|---------------------------|-------------------|----------------------|--------------------|-------------------|
| 4×32^2 | 0.37019_{+3}^{-2} | 0.85_{+5}^{-4} | -0.78_{-4}^{+4} | 1.88_{+4}^{-4} | 1.81_{+4}^{-4} |
| 4×64^2 | 0.2637_{+6}^{-6} | 0.90_{+5}^{-4} | -0.67_{-3}^{+3} | 1.68_{+4}^{-4} | 1.63_{+2}^{-2} |
| 4×128^2 | 0.221_{+3}^{-3} | 0.735_{+7}^{-6} | -0.368_{-14}^{+13} | 1.39_{+10}^{-9} | 1.134_{+2}^{+3} |
| 4×256^2 | 0.218_{+3}^{-3} | 0.73_{+11}^{-8} | -0.33_{-3}^{+2} | 1.39_{+12}^{-10} | 1.02_{+3}^{-3} |
| 6×128^2 | 0.2571_{-5}^{+5} | 0.80_{+2}^{-2} | -0.54_{-3}^{+3} | 1.63_{+16}^{-15} | 1.38_{+4}^{-4} |

TABLE II: As Table I, but for four dimensions.

| Lattice | m_{gribov} [GeV] | a [GeV] | b [GeV] | γ_+ | γ_- |
|-----------------|---------------------------|------------------|----------------------|---------------------|-----------------------|
| 4×46^3 | 0.25_{-2}^{-4} | 1.16_{+6}^{+3} | -0.04_{-8}^{+200} | 1.26_{+11}^{-16} | $0.19_{+0.43}^{+378}$ |
| 6×48^3 | 0.25_{+2}^{-3} | 1.5_{-3}^{+1} | -0.07_{-17}^{+736} | $1.54_{0.05}^{-12}$ | 0.6_{+5}^{+45} |

ever, since the behavior of the Polyakov loop can be derived from the propagators [18], this appears somewhat unlikely, though by far not impossible.

B. Four dimensions

Essentially the same qualitative behavior, though within a different universality class, is expected in four dimensions. The corresponding electric screening mass and its susceptibility are shown in Figure 4. The qualitative picture is the same as in three dimensions. Note, however, that because the critical temperature is about one third lower in four as compared to three dimensions, the physical volumes are about 50% larger here than they would be for the same number of lattice points in three dimensions. Even though our volumes are nevertheless still smaller than in the three-dimensional case, the susceptibility is significantly more peaked, showing that the phase transition leaves a much more significant imprint. However, the peak of the susceptibility is somewhat displaced as compared to the phase transition point. One possible reason could be systematic errors in the scale setting. Other, equally possible, reasons may be statistical fluctuations, finite volume effects or discretization effects. Permitting even only a systematic error of a percent, the correct phase transition temperature is obtained within the total error. Various such sources of systematic uncertainties are further explored in Appendix B.

It is possible to perform the same fits as for the three-dimensional case with the Ansatz (14). The results are given in Table II, and shown in Figure 5. The situation is qualitatively the same as in three dimensions. The resulting critical exponents tend to be somewhat smaller than in three dimensions as expected from universality. The temperature dependence of the electric screening mass below T_c is weaker than before, and in is fact within errors compatible with being essentially constant. With critical scaling, the prediction for its maximal slope at criticality would be roughly $\chi_{\text{max}}^E \propto L^{0.6}$, which would

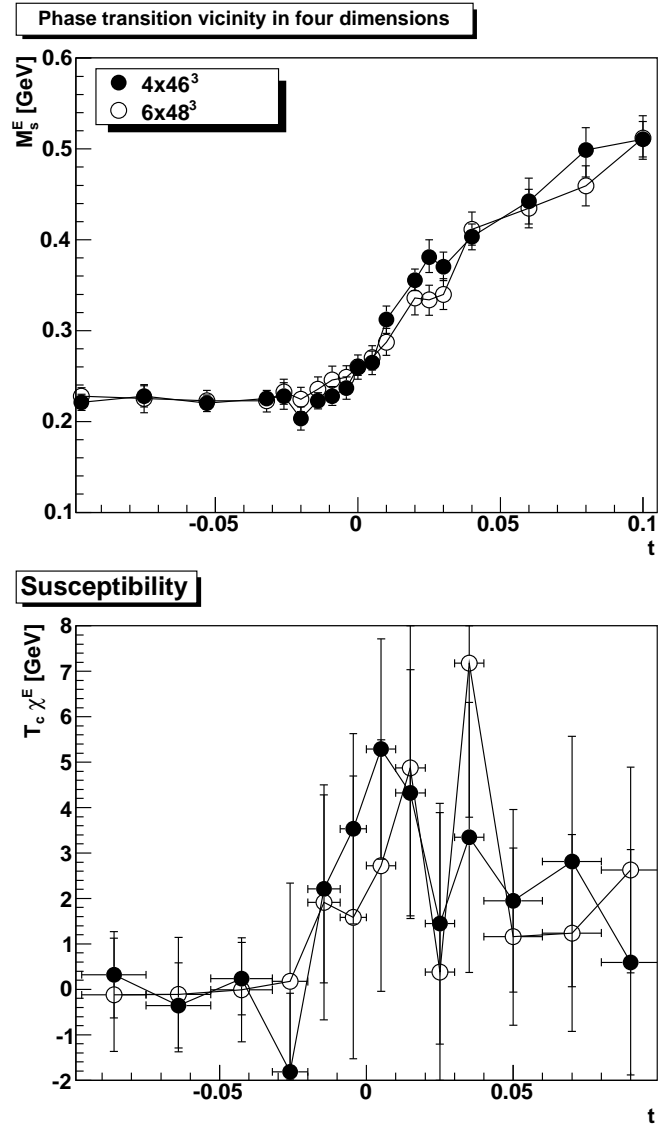


FIG. 4: The electric screening mass (top panel) as a function of the reduced temperature for two different lattice sizes. The bottom panel shows the corresponding susceptibility, where some temperature points have been dropped to reduce the statistical errors.

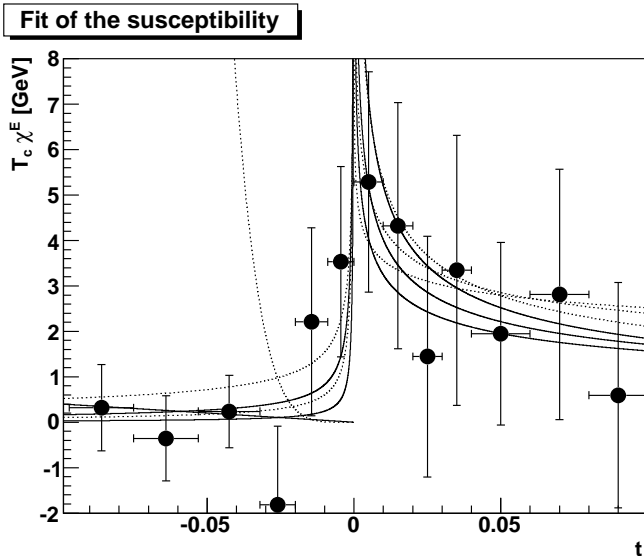
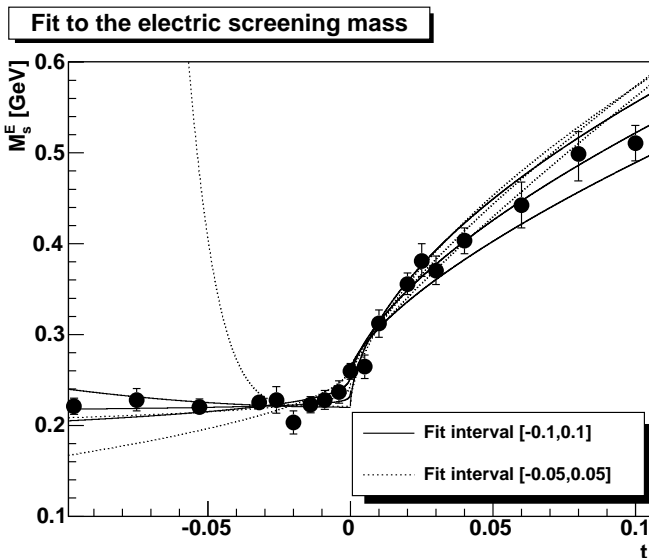


FIG. 5: The quality of the fits compared to the data from the 4×46^3 lattice. The standard fit uses the values from Table I. As an alternative, a fit using only a more restricted reduced temperature interval $[-0.05, 0.05]$ is also shown (dashed line), which yields $\gamma_- = 0.5^{+1.09}_{+6}$ and $\gamma_+ = 1.5^{+3}_{+2}$. Fits have been performed on the screening mass using all data points, and the derivatives have then been calculated analytically.

predict a 25% difference between the two volumes used here. The somewhat stronger volume dependence of the maximum as compared to the three dimensional case might be reflected in Figure 4 but this is well within the present errors still, and thus not significant.

A further point to consider in the four-dimensional case, in contrast to the three-dimensional one, is renormalization. In three dimensions the gluon propagator is finite, and no renormalization is necessary. This is not the case in four dimensions. As a consequence, the screening mass, in contrast to a pole mass, is renormalization-scale dependent [30]. Here, the renor-

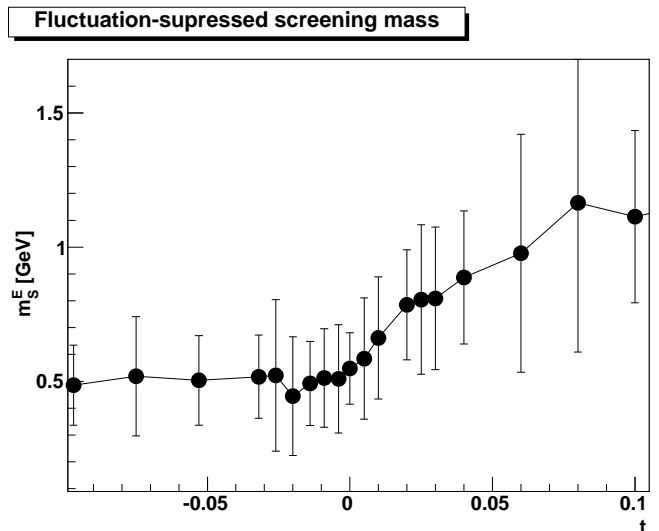


FIG. 6: The fluctuation of the screening mass (15) in four dimensions from the 4×46^3 lattice.

malization is performed by requiring $\mu^2 D_L(\mu, T) = 1$ at $\mu = 2$ GeV. However, this is problematic for two reasons. First, this introduces a temperature dependence of the renormalization constant. Secondly, the renormalization prescription for the gluon propagator in Landau gauge is linked to the one for the ghost propagator which might lead to a potential inconsistency, since also the ghost propagator can acquire a temperature-dependent renormalization. In the present case, however, these effects can be estimated and are found to be well within the statistical errors, see Appendix B 2.

C. Alternative observables

Since in both three and four dimensions the gluon propagator does not show a behavior which can immediately be interpreted as a pure critical behavior, a natural question might be whether one can suppress the influence of non-thermal contributions depending on whether they are due to discretization, finite volume artifacts, genuine quantum effects, or the Gribov mass as mentioned.

For this purpose the fluctuations of the screening mass can be used, which are defined as

$$m_s = \frac{1}{\sqrt{D^S(0)}} \quad (15)$$

$$D^S(0) = \langle D(0) \rangle - \langle \sqrt{D(0)} \rangle^2.$$

This essentially amounts to determining the pure fluctuating part.

The resulting screening mass for the four-dimensional case is shown in Figure 6. There are a number of observations which can be made, despite the significantly increased statistical uncertainty. First, the global features

of the screening mass are maintained. Secondly, even after removing the non-fluctuating part there is a non-zero baseline, which implies that the Gribov mass from the gauge fixing is present even in the fluctuations, though, of course its infinite volume behavior cannot be inferred from these results. Thirdly, the slope again appears to increase at the phase transition, which is not a statistically very sound result at present, however. Nonetheless, the behavior is suggestive, and this would imply a similar phase transition signal also in the fluctuations.

In relation to the original goal of isolating critical behavior, however, there is no sign of improvement as compared to the screening mass.

A second alternative would be the magnetic screening mass. From the results in [18] and the results shown in Appendices A and C, it can already be inferred that it will not exhibit a strong signal of the phase transition. Indeed, a more detailed investigation of its susceptibility shows that, if there is any signal of the phase transition encoded in the magnetic screening mass at all, it is certainly substantially weaker than that in the electric one. The same applies to the gauge-fixing sector in form of the Faddeev-Popov ghosts.

IV. A NOTE ON FOUR-DIMENSIONAL $SU(3)$ YANG-MILLS THEORY

The physically more relevant case of four-dimensional $SU(3)$ Yang-Mills theory exhibits a (weak) first-order transition [52]. It has previously been studied with functional methods [12–17, 30–34, 38, 53–56] and on the lattice [18, 22, 30]. The correlation length remains finite, and one does not expect critical scaling. In principle, one should be able to study the finite-size scaling with integer exponents characteristic of first-order transitions which is rather expensive to investigate in lattice simulations, however.

Here we analyze the data from [18, 30] supplemented by additionally generated temperature points and with improved statistics in a closer window around the transition for comparison. This leads to an electric screening mass and a susceptibility in four-dimensional $SU(3)$ as shown in Figure 7. There is no significant temperature dependence below T_c in the range considered here. The constant value serves as the baseline in our fit. Above T_c we allow a temperature dependence of a form which is typical for a first-order transition in addition to the constant contribution. With these assumptions we observe that the data in the reduced temperature interval $[-0.1, 0.1]$ is well described by a fit of the form

$$M_s^E = m_{\text{gribov}} + \theta(t) a \sqrt{\delta + t}, \quad (16)$$

with parameters $m_{\text{gribov}} = 0.222_{-5}^{-3}$ GeV, $a = 0.7_{-1}^{-4}$ GeV, and $\delta = 0.06_{+37}^{-4}$.

The data provides rather clear indication that a pronounced jump forms at the transition characteristic of its

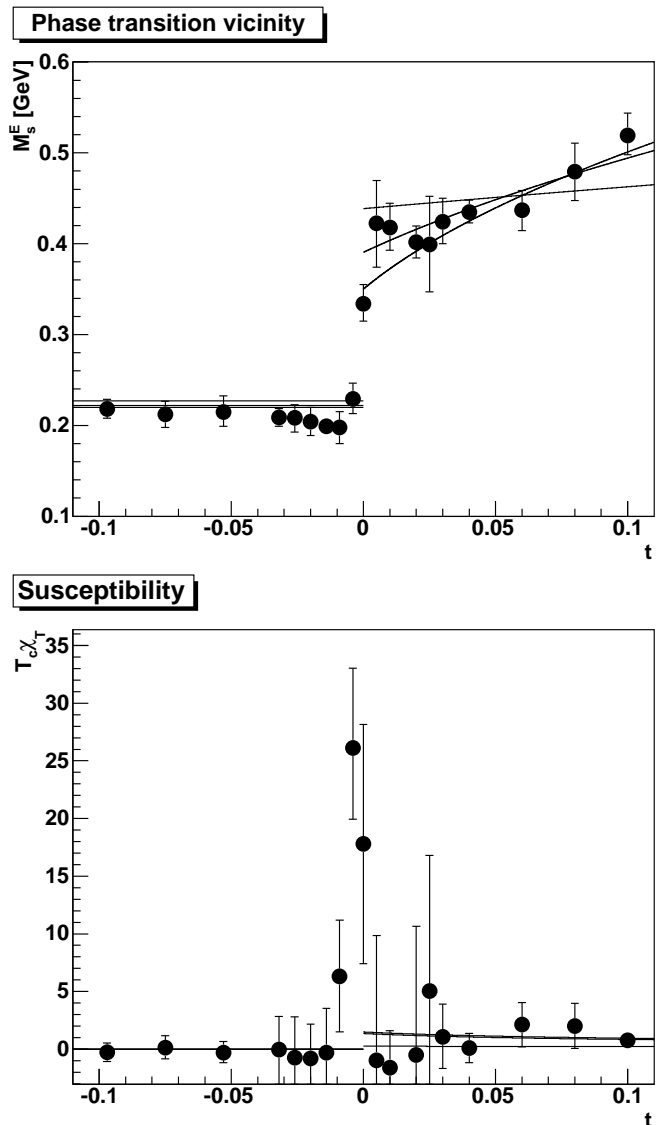


FIG. 7: The electric screening mass and susceptibility for four-dimensional $SU(3)$ Yang-Mills theory on 4×34^3 lattices close to the phase transition, compared to a fit of type (16).

first-order nature. A much more detailed analysis especially of the finite volume behavior of these results will be necessary to substantiate whether a discontinuity in the electric screening mass develops in the infinite volume limit or not. The fact that the transition is only weakly first order makes such an analysis particularly demanding. At present we can conclude, however, that the behavior looks significantly different from the second-order cases discussed in Section III. An emerging discontinuity at the phase transition appears to be indicative of a sensitivity of the longitudinal gluon propagator to the order of the transition. One should nevertheless be wary of lattice artifacts [22] in this exploratory study also.

V. CONCLUSIONS AND OUTLOOK

In summary, we argue that critical behavior of the confinement-deconfinement phase transition of pure Yang-Mills theory should be reflected in the longitudinal gluon propagator, in particular, in the electric screening mass. Our data shows in all cases, for $SU(2)$ and $SU(3)$, that the phase transition can be clearly identified by a peak in its temperature derivative. Although it turns out to be rather difficult to disentangle a singular critical contribution to the electric screening mass from a regular one, which is presumably predominantly a Gribov copy effect, it seems that there is such a contribution in $SU(2)$, and that this contribution changes when going from three to four dimensions in a way consistent with the change from the $2d$ to the $3d$ Ising universality class. Our results for the critical exponents are still somewhat off, however, which might be mainly due to an insufficient way of isolating the corresponding contributions. Whether our qualitative findings will finally be backed by a more quantitative analysis on the basis of universality arguments, including a verification of the expected finite-size scaling, as it is well established for various other observables, will have to await further study.

In comparison, the electric screening mass of pure $SU(3)$ in four dimensions appears to show the discontinuity indicative of the first-order phase transition there. This seems to indicate that the electric gluon propagator is sensitive to the order of the transition, likewise.

To ultimately clarify all this will require both substantially larger spatial volumes as well as finer discretizations. It will be important to further pursue this for two reasons: One is that identifying critical behavior in this simplest of observables will improve our understanding of the driving mechanisms behind critical behavior and the order of the phase transition in general. Secondly, this clarification is of great interest in the construction of realistic truncation schemes for functional methods which have the potential of providing a genuine first-principle approach to describe full QCD with various quark flavors and masses at finite temperature and density [7].

Thus, to further pursue these investigations is of prime importance in our efforts to combine both numerical lattice and functional continuum methods for a reliable determination of the QCD phase diagram.

Acknowledgments

We are grateful to Christian S. Fischer and Michael Müller-Preussker for a critical reading of the manuscript.

This work is supported by the Helmholtz Alliance HA216/EMMI and the Helmholtz International Center for FAIR within the LOEWE program of the State of Hesse. A.M. was supported by the FWF under grant number M1099-N16 and by the DFG under grant number MA 3935/5-1. L.v.S. received additional support from the Helmholtz Association, Grant VH-NG-

332, and the European Commission, FP7-PEOPLE-2009-RG, No. 249203. D.S. acknowledges support by the Landesgraduiertenförderung Baden-Württemberg via the Research Training Group ‘‘Simulational Methods in Physics’’. The numerical simulations were carried out on bwGRiD (<http://www.bw-grid.de>), member of the German D-Grid initiative, on the computer cluster of the ITP, University of Heidelberg, and the HPC clusters of the Universities of Graz and Jena. The ROOT framework [57] has been used in this project.

Appendix A: Full momentum dependence

Besides the critical behavior manifest at zero momentum also the full momentum dependence of the propagators is important, both for combining with functional methods as well as to estimate the reliability of other approximation techniques, like e. g. hard-thermal-loop calculations close to the phase transition.

Hence, in this appendix the full momentum dependence of both parts of the propagator, the electric and the magnetic one, for the zeroth Matsubara frequency will be presented. Higher Matsubara frequencies can then be approximated rather accurately with this information [18]. Results for the Faddeev-Popov ghost can be found elsewhere [18, 19, 30, 58].

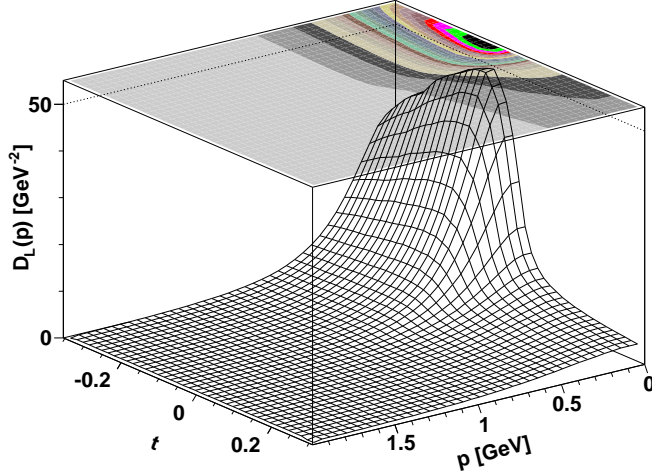
The results in three dimensions are shown in figure 8 for the 4×128^2 lattice. For four dimensions the results for the 6×48^3 lattice are shown in figure 9. The results for the 4×46^3 lattice can be found in [18]. For both dimensions, the results are qualitatively similar, up to the differences present already at zero temperature. In particular, the abrupt change in the electric screening mass discussed in the main text finds its echo at finite momentum. The magnetic propagator shows no pronounced dependence on the temperature, except for a general suppression.

It is an interesting observation that the smoothness of the electric screening mass in three dimensions compared to four dimensions also surfaces in the finite momentum behavior. This again can be interpreted as a sign that Yang-Mills theory in four dimensions is ‘closer’ to a first order transition than three dimensions, as is known from other observables.

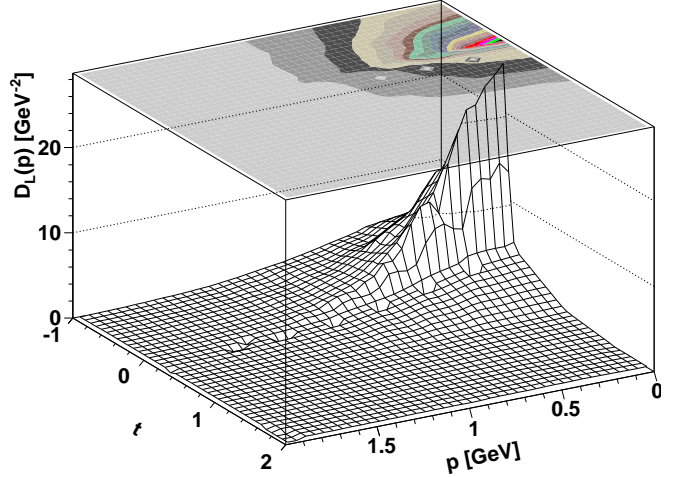
Appendix B: Systematic errors

Calculations like the present ones are sensitive to various systematic errors, as has been pointed out repeatedly [18–22]. In the following various such errors will be discussed in turn, including the scale setting, renormalization, finite-volume effects and aspect ratio issues.

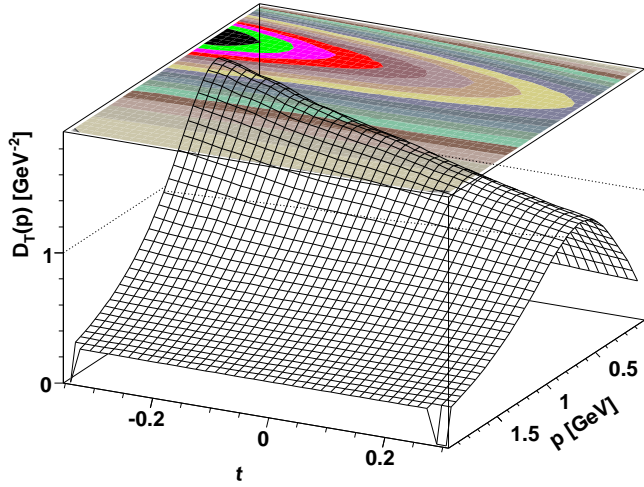
Electric gluon propagator in three dimensions



Electric gluon propagator in four dimensions



Magnetic gluon propagator in three dimensions



Magnetic gluon propagator in four dimensions

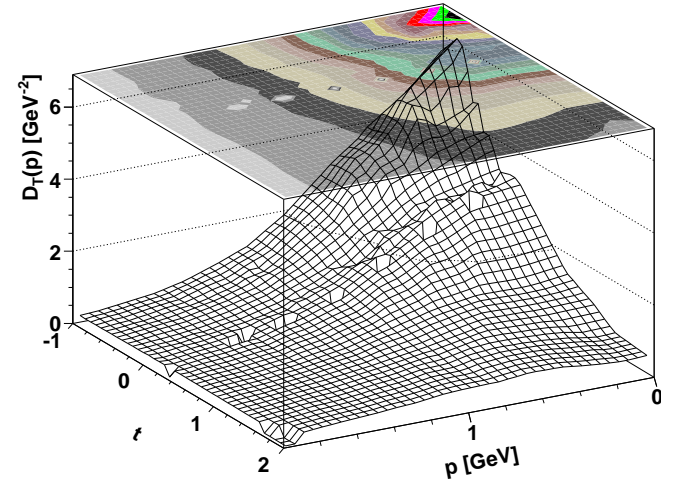


FIG. 8: The full momentum dependence of the zero-mode electric (top panel) and magnetic (bottom panel) gluon propagator in three dimensions on a 4×128^2 lattice.

1. Scale setting

The scale in the present calculations has been set in four dimensions using an interpolation formula of the type,

$$a\sqrt{\sigma} = \frac{c_1}{\beta} + \frac{c_2}{\beta^2} + \frac{c_3}{\beta^3} + \frac{c_4}{\beta^4}.$$

with σ , the string tension, set to $(440\text{MeV})^2$, and where the coefficients have been fitted to the results from [50], yielding $c_1 = 31.9$, $c_2 = -237$, $c_3 = 574$, and $c_4 = -444$. However, since reduced temperatures of size 0.01 have been included in the calculation, this setting maybe too imprecise. Using data from [59], different values for the coefficients have been obtained as $c_1 = 33.6$, $c_2 = -249$, $c_3 = 599$, and $c_4 = -461$. In this case, the critical β was

FIG. 9: The full momentum dependence of the zero-mode electric (top panel) and magnetic (bottom panel) gluon propagator in four dimensions. To extend the temperature range outside the $[-0.1, 0.1]$ interval additional lattice sizes have been used, which are chosen to have an approximately constant number of lattice points as the 6×48^3 lattices in this reduced temperature range. Dips along the $t = 0$ line are artifacts from the graphical interpolation routine.

determined more precisely as $\beta = 2.2986$, instead of $\beta = 2.299$, as used in the main part of the text. However, this leads only to a shift in t of the order of 0.01, i. e., reduced temperatures in the main text should be taken to have a systematic uncertainty of ± 0.01 . This accommodates the shift of the peak of the susceptibilities in figure 4 compared to $t = 0$. Similar comments apply, of course, to the three-dimensional case.

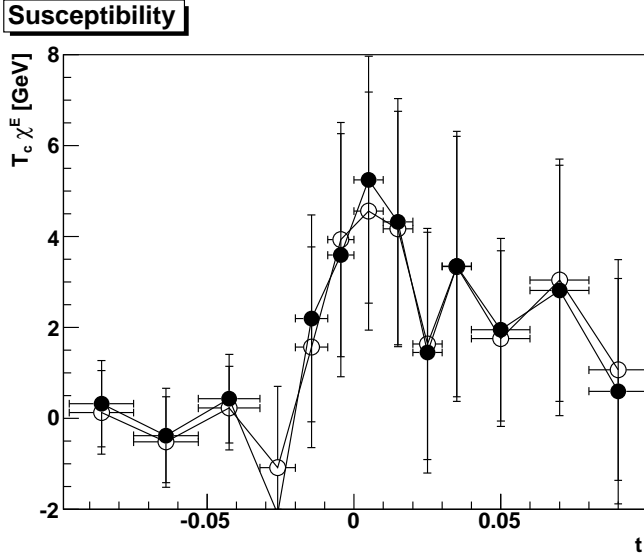
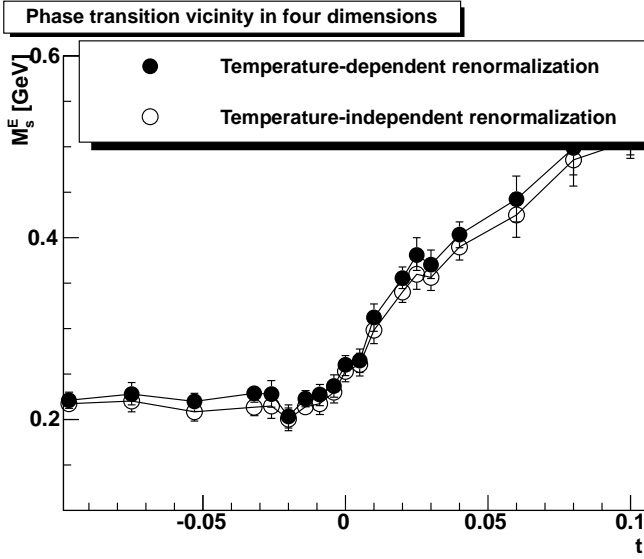


FIG. 10: The electric screening mass and susceptibility determined using a temperature-dependent renormalization prescription, as in the main text, and a temperature-independent renormalization prescription.

2. Renormalization

In four dimensions, the propagators have to be renormalized. As a consequence, also the screening mass is renormalized by the same wave-function renormalization factor. In the main text, this is done at each temperature individually at 2 GeV. Of course, since finite temperature is not introducing any new divergences [60], it is also possible to renormalize once and for all at zero temperature. However, since the renormalization constants are both potentially volume-dependent and not available for all β values investigated, this has not been done here.

To assess the relevance of renormalization, it is shown in figure 10 the effect of renormalizing only once at zero

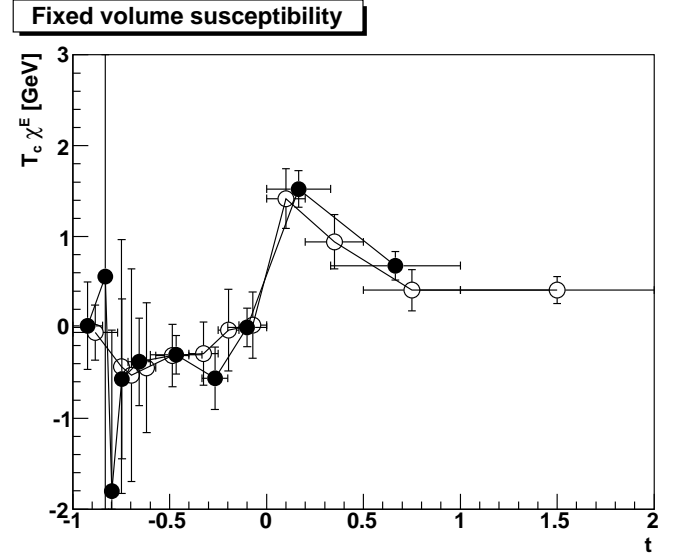
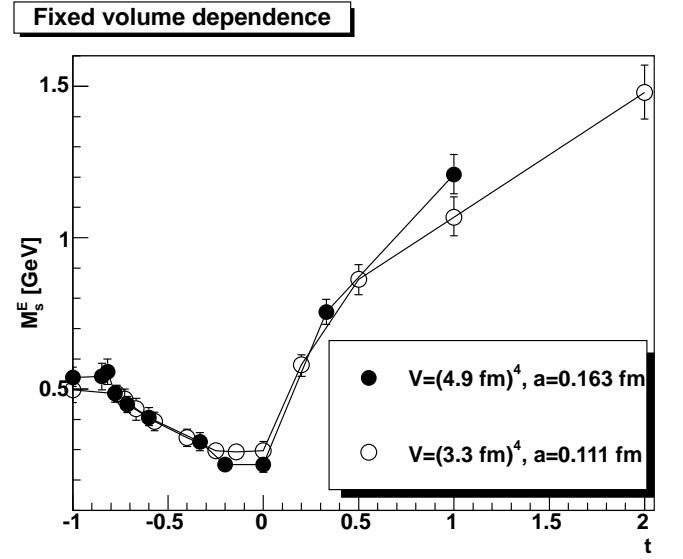


FIG. 11: The electric screening mass and susceptibility as a function of the reduced temperature at fixed spatial volume for two different volumes.

temperature for the 4×46^3 lattice. Here, the β dependence of the renormalization constants is ignored, given that it is expected to be only logarithmic in the scaling regime. The result show indeed no change within statistical errors. This was expected, as at a momentum of 2 GeV temperature effects are still rather small. This may change at larger temperatures, but is not relevant for the present purpose.

3. Finite volume effects

In the main text, the spatial volume was not kept fixed, but small variations have been permitted to obtain a very dense mesh of temperatures around the critical one. In

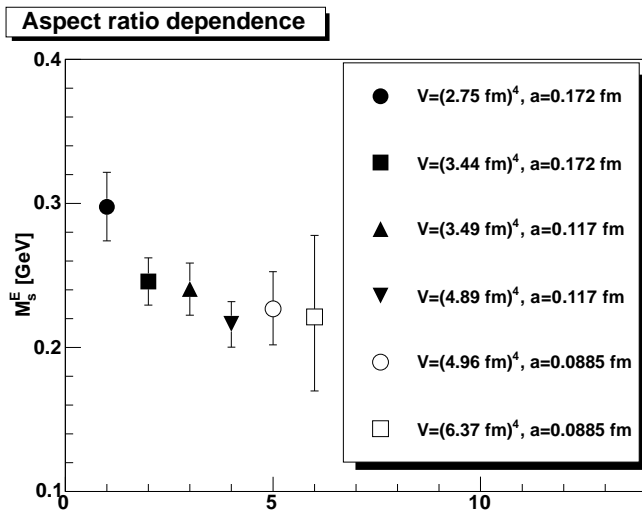


FIG. 12: The electric screening mass as a function of the aspect ratio at $T = 0.95T_c$. The aspect ratios from left to right are, respectively, 1:4, 1:5, 1:5, 1:7, 1:7, and 1:9.

particular, the spatial volumes at very low temperatures and very high temperatures are quite different. To assess the influence of this effect, the electric screening mass and susceptibility is shown at fixed spatial volume in figure 11.

As is visible, the overall generic behavior over the whole temperature range is not significantly altered when using a fixed instead of a varying spatial volume. However, as has already been observed in other calculations [21], it is visible that a finer lattice seems to increase the plateau directly before the phase transition. Of course, in the present case neither the temperature mesh, nor the spatial volumes, are exceptionally large. Therefore, this should be taken only as an indication, and requires further study.

4. Aspect ratio

As already indicative in the discussion of the finite volume effects, also the aspect ratio and the temporal discretization play a significant role. In figure 12 the electric screening mass at a fixed temperature is shown for a number of different spatial volumes and aspect ratios. In the figure, the aspect ratio increases from left to right, approaching the infinite-volume and continuum limit such that the temperature extension remains finite, while the spatial extension diverges. It is visible that at small aspect ratios and volumes a significant dependence on these two parameters exist. However, towards the infinite-volume and continuum limit, this dependency quickly diminishes, if the limit is taken in the presented order, though the statistical error bars are rather large. The final value is in agreement with the one obtained in the main text. In contrast, at fixed aspect ratio and

spatial volume a much larger impact of going to the continuum limit has been found [19, 21], indicating that the different approaches towards the desired limit have to be investigated carefully.

Appendix C: Statistical errors

The assessment of the quality of fits presented in the main text is a rather complicated problem. Usual χ^2 checks can only be expected to give a reliable estimate if the fit form is linear, but the present one is non-linear, non-analytic, and non-continuously differentiable, and in the case of SU(3) not even continuous. To estimate the statistical error of the fit thus instead a comparison to a null hypothesis is used. This null hypothesis is the absence of any signal of the phase transition, i. e., a trivial linear behavior

$$M_s^E(t) = m_0 + a(1 + t). \quad (\text{C1})$$

For a quantity not influenced strongly by the phase transition this is an adequate description, as is shown in case of the magnetic screening mass in figure 13.

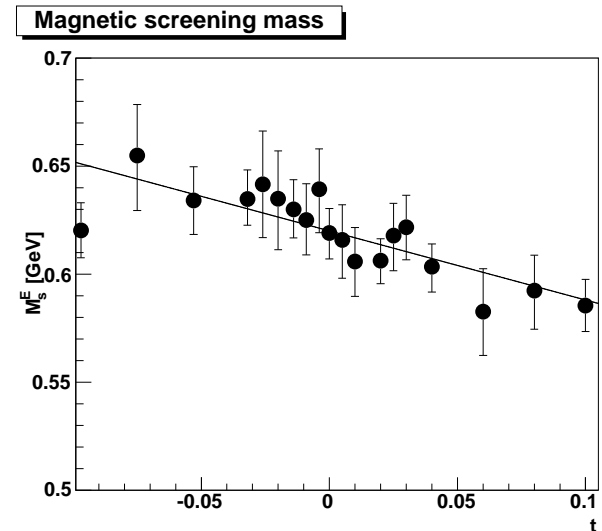


FIG. 13: The magnetic screening mass on the 4×46^3 lattice close to the phase transition temperature compared to a linear fit.

To estimate the error, the results for the electric screening mass have also been fitted to the formula (C1). Then, instead of using the average values for the electric screening mass, a value within the 67% confidence interval for each temperature point was chosen such that it was closest to the fitted linear behavior. Then these points were fitted again within the fit ansatz (12). Since the ansatz (12) contains also this null hypothesis, this gives exponents as close as possible to the null hypothesis. To estimate an opposite error, the fluctuation were performed towards as far away as possible from the null hypothesis

(C1). These two fits gave two further fit parameters. In the tables I and II the deviation of the fit parameters towards the null hypothesis is set as a subscript, while those as far away from the null hypothesis as possible are set as superscripts. These results have been used in the figures 3 and 5. In the four-dimensional case in the low-temperature phase the uncertainties in the fits is quite significant, a consequence of the compatibility with

a constant within errors. Thus fits with free pre-factor and exponent can turn out to be optimal by combining very extreme combinations of both. The result should thus be rather interpreted as that the low-temperature behavior is within errors compatible with a constant.

In the SU(3) case in figure 7 the error for the fit was determined in the same way.

-
- [1] P. Jacobs *et al.*, (2007), 0705.1930.
- [2] A. Andronic *et al.*, Nucl.Phys. **A837**, 65 (2010), 0911.4806.
- [3] S. Leupold *et al.*, Lect.Notes Phys. **814**, 39 (2011).
- [4] HotQCD collaboration, A. Bazavov and P. Petreczky, J.Phys.Conf.Ser. **230**, 012014 (2010), 1005.1131.
- [5] M. Cheng *et al.*, Phys. Rev. **D81**, 054510 (2010), 0911.3450.
- [6] Wuppertal-Budapest Collaboration, S. Borsanyi *et al.*, JHEP **1009**, 073 (2010), 1005.3508.
- [7] J. M. Pawłowski, AIP Conf.Proc. **1343**, 75 (2010), 1012.5075.
- [8] S. R. Edwards, A. Sternbeck, and L. von Smekal, PoS **LATTICE2010**, 275 (2010), 1012.0768.
- [9] P. de Forcrand and L. von Smekal, Phys.Rev. **D66**, 011504 (2002), hep-lat/0107018.
- [10] L. von Smekal, S. R. Edwards, and N. Strodthoff, PoS **LATTICE2010**, 292 (2010), 1012.0408.
- [11] N. Strodthoff, S. R. Edwards, and L. von Smekal, PoS **LATTICE2010**, 288 (2010), 1012.0723.
- [12] J. Braun, H. Gies, and J. M. Pawłowski, Phys. Lett. **B684**, 262 (2010), 0708.2413.
- [13] F. Marhauser and J. M. Pawłowski, (2008), 0812.1144.
- [14] J. Braun, A. Eichhorn, H. Gies, and J. M. Pawłowski, Eur.Phys.J. **C70**, 689 (2010), 1007.2619.
- [15] J. Braun, L. M. Haas, F. Marhauser, and J. M. Pawłowski, Phys. Rev. Lett. **106**, 022002 (2011), 0908.0008.
- [16] C. S. Fischer, Phys. Rev. Lett. **103**, 052003 (2009), 0904.2700.
- [17] C. S. Fischer and J. A. Müller, Phys. Rev. **D80**, 074029 (2009), 0908.0007.
- [18] C. S. Fischer, A. Maas, and J. A. Müller, Eur. Phys. J. **C68**, 165 (2010), 1003.1960.
- [19] A. Cucchieri, A. Maas, and T. Mendes, Phys. Rev. **D75**, 076003 (2007), hep-lat/0702022.
- [20] V. G. Bornyakov and V. K. Mitrjushkin, Phys.Rev. **D84**, 094503 (2011), 1011.4790.
- [21] A. Cucchieri and T. Mendes, PoS **FACESQCD**, 007 (2011), 1105.0176.
- [22] R. Aouane *et al.*, (2011), 1108.1735.
- [23] P. De Forcrand and L. Von Smekal, Nucl.Phys.Proc.Suppl. **106**, 619 (2002), hep-lat/0110135.
- [24] C. Gattringer, Phys. Rev. Lett. **97**, 032003 (2006), hep-lat/0605018.
- [25] F. Synatschke, A. Wipf, and C. Wozar, Phys.Rev. **D75**, 114003 (2007), hep-lat/0703018.
- [26] E. Bilgici, F. Bruckmann, C. Gattringer, and C. Hagen, Phys.Rev. **D77**, 094007 (2008), 0801.4051.
- [27] B. Zhang, F. Bruckmann, C. Gattringer, Z. Fodor, and K. K. Szabo, AIP Conf.Proc. **1343**, 170 (2011), 1012.2314.
- [28] E. Bilgici *et al.*, Few Body Syst. **47**, 125 (2010), 0906.3957.
- [29] C. S. Fischer, J. Luecker, and J. A. Mueller, Phys.Lett. **B702**, 438 (2011), 1104.1564.
- [30] A. Maas, (2011), 1106.3942.
- [31] A. Maas, J. Wambach, and R. Alkofer, Eur. Phys. J. **C42**, 93 (2005), hep-ph/0504019.
- [32] A. Maas, J. Wambach, B. Grüter, and R. Alkofer, Eur. Phys. J. **C37**, 335 (2004), hep-ph/0408074.
- [33] B. Grüter, R. Alkofer, A. Maas, and J. Wambach, Eur. Phys. J. **C42**, 109 (2005), hep-ph/0408282.
- [34] I. Zahed and D. Zwanziger, Phys. Rev. **D61**, 037501 (2000), hep-th/9905109.
- [35] A. Cucchieri, F. Karsch, and P. Petreczky, Phys. Lett. **B497**, 80 (2001), hep-lat/0004027.
- [36] A. Cucchieri, F. Karsch, and P. Petreczky, Phys. Rev. **D64**, 036001 (2001), hep-lat/0103009.
- [37] F. Karsch and J. Rank, Nucl. Phys. Proc. Suppl. **42**, 508 (1995).
- [38] M. N. Chernodub and V. I. Zakharov, Phys. Rev. Lett. **100**, 222001 (2008), hep-ph/0703167.
- [39] L. Fister and J. M. Pawłowski, (2011), 1112.5440.
- [40] V. N. Gribov, Nucl. Phys. **B139**, 1 (1978).
- [41] A. Pelissetto and E. Vicari, Phys.Rept. **368**, 549 (2002), cond-mat/0012164.
- [42] A. Sternbeck, L. von Smekal, D. B. Leinweber, and A. G. Williams, PoS **LAT2007**, 340 (2007), 0710.1982.
- [43] I. L. Bogolubsky, E. M. Ilgenfritz, M. Müller-Preussker, and A. Sternbeck, Phys. Lett. **B676**, 69 (2009), 0901.0736.
- [44] A. Cucchieri and T. Mendes, Phys. Rev. Lett. **100**, 241601 (2008), 0712.3517.
- [45] A. Cucchieri and T. Mendes, Phys. Rev. **D78**, 094503 (2008), 0804.2371.
- [46] A. Cucchieri, A. Maas, and T. Mendes, Phys. Rev. **D74**, 014503 (2006), hep-lat/0605011.
- [47] A. Cucchieri and T. Mendes, PoS **LAT2007**, 297 (2007), 0710.0412.
- [48] I. Bogolubsky, E. Ilgenfritz, M. Muller-Preussker, and A. Sternbeck, PoS **LAT2007**, 290 (2007), 0710.1968.
- [49] M. J. Teper, Phys. Rev. **D59**, 014512 (1999), hep-lat/9804008.
- [50] J. Fingberg, U. M. Heller, and F. Karsch, Nucl. Phys. **B392**, 493 (1993), hep-lat/9208012.
- [51] S. Edwards and L. von Smekal, Phys.Lett. **B681**, 484 (2009), 0908.4030.
- [52] F. Karsch, Lect. Notes Phys. **583**, 209 (2002), hep-lat/0106019.
- [53] J. Braun, Eur. Phys. J. **C64**, 459 (2009), 0810.1727.

- [54] J. Braun and H. Gies, Phys. Lett. **B645**, 53 (2007), hep-ph/0512085.
- [55] C. D. Roberts and S. M. Schmidt, Prog. Part. Nucl. Phys. **45**, S1 (2000), nucl-th/0005064.
- [56] D. Zwanziger, Phys. Rev. **D76**, 125014 (2007), hep-ph/0610021.
- [57] R. Brun and F. Rademakers, Nucl. Instrum. Meth. **A389**, 81 (1997).
- [58] A. Maas, unpublished.
- [59] B. Lucini, M. Teper, and U. Wenger, JHEP **01**, 061 (2004), hep-lat/0307017.
- [60] A. K. Das, *Finite temperature field theory* (World Scientific, Singapore, 1997), Singapore, Singapore: World Scientific (1997) 404 p.